AIAA JOURNAL
Vol. 32, No. 12, December 1994

Investigation of the Free Vibration of a Rectangular Membrane

R. K. Singhal*
Canadian Space Agency, Ottawa, Ontario K2H 8S2, Canada
D. J. Gorman†
University of Ottawa, Ottawa, Ontario K1N 6N5, Canada
J. M. Crawford‡
Dynacon Enterprises Ltd., Downsview, Ontario M3H 5T5, Canada
and
W. B. Graham§
Software Systems Engineering, Ottawa, Ontario K1V 8B9, Canada

An experimental and theoretical study of the free vibration of a rectangular membrane is described. The membrane has an unidirectional tension imposed through rigid transverse bars attached near the extremities of the membranes along the short edges. The results of experimental tests conducted in air and in vacuum are reported. These are compared with theoretical frequencies computed by both a finite element model and a continuum mechanical model. Good agreement is obtained. Further studies involving membranes with additional complicating factors are described briefly.

Nomenclature

A_{mB} = ratio of batten mass to quarter membrane mass
A_{MI} = $I/\rho a^3 b$
a, b = dimensions of quarter membrane
c = $\sqrt{T/\rho}$
I = moment of inertia of quarter membrane batten about one of its extremities
k = number of terms utilized in series expansion
P/a = force per unit length exerted on batten by membrane
T = uniaxial tension in membrane
v = distance from fixed boundary to batten
w = membrane lateral displacement
x, y = spatial coordinates used on quarter membrane

Introduction

THE use of tensioned rectangular membranes in space systems has given rise to a number of challenging technological problems. As currently envisioned in a space-based radar application, these membranes would be launched in a wrapped up (stowed) condition. Subsequently, they would be unwrapped and deployed in a tensioned configuration. As part of the design, performance evaluation, and testing process, the natural frequencies and mode shapes of these membranes must be clearly established. This task is made difficult because of a number of complications which characterize the membrane itself as well as the manner in which it will be tensioned in space. Some of these complications and/or characteristics are as follows.

1) Because of the need to stow a large membrane into a compact package for flight, the membrane will be divided into segments joined by simply connected boundaries (running parallel to its long central axis).

2) Each segment will be given equal initial tension in the direction of this long axis, the tension being applied to the individual segments by a pair of rigid transverse bars.

3) The bars will be attached to fixed boundaries by means of short tensioning strings or cables.

4) The lateral surface of the membrane will have attached to it a closely spaced grid of radio-frequency (rf) modules.

5) Ground tests must be carried out with the plane of the membrane in the vertical plane and under vacuum conditions. Because of the rf module attachments the effective mass per unit area of the structure will be sufficiently high so that variation in tension due to gravity cannot be neglected.

6) The rf module attachments add sufficient stiffness to the membrane so that the effects of its flexural rigidity on free vibration cannot be neglected.

An example of a structure exhibiting these characteristics is the test article developed for the lens antenna demonstration development (LADD) program, which is a "coupon" representative of a proposed space system.[1]

The work described in this paper does not seek a solution dealing with all of these complications. A search of the literature reveals that little assistance, beyond the classical membrane theory, is to be found there. Accordingly, as a first phase of a more general investigative program, an experimental and theoretical study of the free vibrational behavior of a membrane composed of one section and tensioned by attached bars as just described, but without the presence of the attached rf modules, was performed. Furthermore, it was considered that membrane structures would be amenable to solution by continuum mechanical methods (CMM); therefore, in addition to modeling the membrane by way of the finite element method (FEM) a CMM model was developed.

The objectives of the work were to establish and demonstrate for membranes: 1) the practicality of modal testing using a noncontact measurement system (laser vibrometer) by determining well-defined modal parameters, 2) appropriate excitation methods in tests, 3) the significance of aerodynamics effects in tests, and 4) that CMM models are appropriate.

This work was in general support of preparatory work for modal testing of the LADD test article (LTA). This paper describes the test article designed and built for testing, the CMM analysis performed, the FEM approach, the modal tests conducted, and finally compares the results.

Description of Experimental Model

A diagram of the membrane test article is shown in Fig. 1. Figure 2 is a photograph of the same membrane. The membrane consists of a rectangular section of Kapton, 0.914 m × 2.286 m (3 ft × 7.5 ft)

Received Jan. 19, 1994; revision received June 8, 1994; accepted for publication June 8, 1994.

*Senior Structural Dynamicist, David Florida Laboratory, P. O. Box 11490, Station H.
†Professor, Department of Mechanical Engineering.
‡Junior Research Engineer, 5050 Dufferin St., Suite 222.
§Senior Aerospace Engineer, 2487 Kaladar.

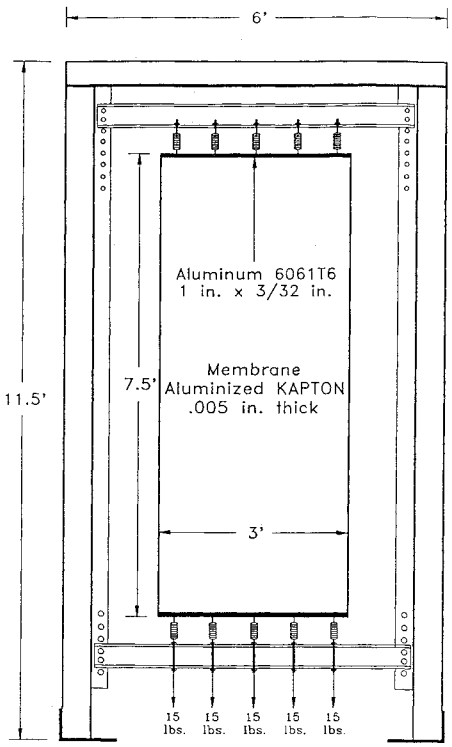

Fig. 1 Diagram of membrane test article.

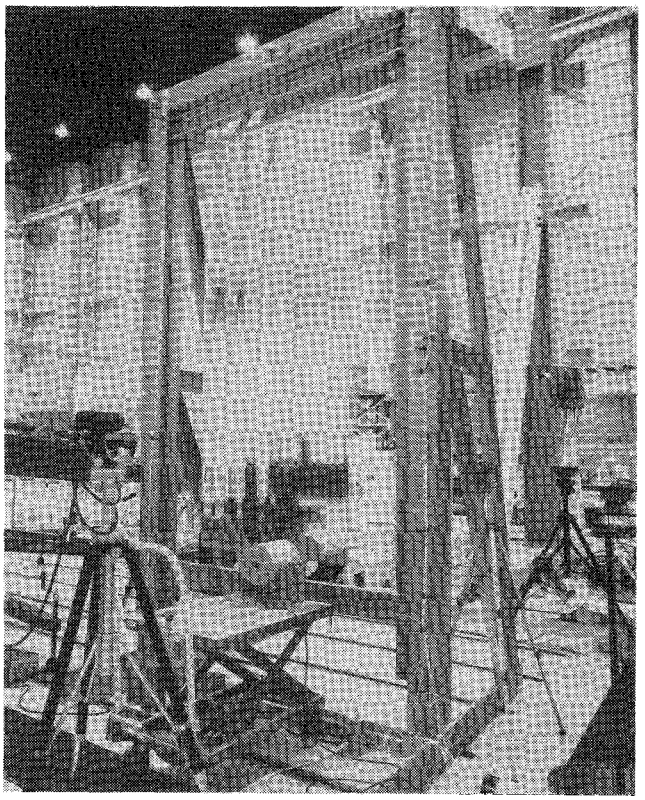

Fig. 2 Photograph of the test setup with membrane mounted on the frame.

of 0.125 mm (0.005 in.) thickness, with an area factor of 5.5 m^2/kg (27 ft^2/lb). The horizontal extremities of the membrane terminate at aluminum battens. Each batten is composed of two aluminum strips 25.4 mm (1.00 in.) wide × 2.38 mm (0.0937 in.) thick. The strips are bonded to either face of the membrane thereby forming a sandwich joint or batten. The aluminum battens are attached to the upper extremity of the aluminum support frame by means of five equally spaced springs as seen in the photograph (Fig. 2). A corresponding set of springs is attached to the lower bar. The lower wire extensions of these springs pass through circular passages with locking devices.

In preparation for tensioning of the membrane, small weight containers are attached to the lower extremities of each lower spring. Small equal weights are added successively to each container until the desired end load, and hence the desired tension, is induced in the membrane. The locking devices are engaged, leaving the membrane with the desired tension and boundary conditions. A succession of frequency tests are subsequently performed to verify that no tension relaxation has occurred due to creep of the membrane material.

Experimental tests to establish the free vibration frequencies and mode shapes of the membrane assembly of Fig. 2 were conducted both in air and in vacuum.

Theoretical Analysis

Two analytical models were developed. One solution was sought by means of an extension of classical analytical solutions, that is, using CMM solutions. The other solution was based on the FEM approach. In-house finite element program was employed to obtain an FEM solution.

Continuum Mechanical Methods Approach

For the present analysis, gravitational acceleration is assumed to be zero. In the mathematical model of the CMM approach, further simplification is introduced. It is assumed that the short springs connecting the transverse bars to the upper and lower fixed boundaries are replaced by regular membrane material. Since the spring lengths are very short, in comparison to the overall membrane length, this slight compromise in the model is considered to have little effect on the computed behavior. It contributes significantly to simplifying the analysis.

Fully Symmetric Modes

This family of modes is defined to be symmetric with respect to the central axes of the membrane. In view of this symmetry only one-quarter of the membrane as shown in Fig. 3 need be analyzed. Arbitrarily, the upper right quadrant of the membrane is selected. Because of symmetry, slope taken normal to the interior edges of this quarter of the membrane will be everywhere zero. This zero-slope condition is indicated by small pairs of circles adjacent to these edges. The analytical procedure followed is similar to that described in Ref. 2.

During vibratory motion, the membrane displacement is a function of the coordinates y only (see Fig. 4). For convenience, the membrane of the figure is divided into two segments with a common boundary along the line of contact of the attached batten.

The membrane battens, for this analysis, are assumed to be rigid. During vibratory motion, the battens undergo harmonic translation motion only, driven by a uniform force of amplitude P/a per unit length along the membrane.

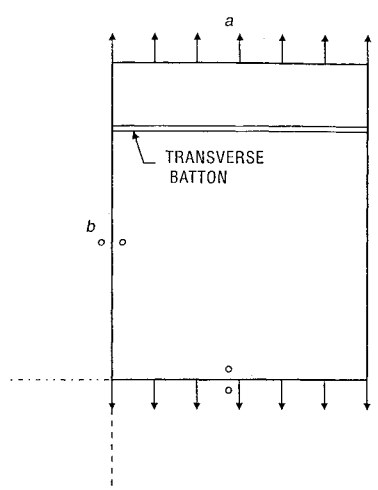

Fig. 3 Upper right quarter of membrane under analysis.

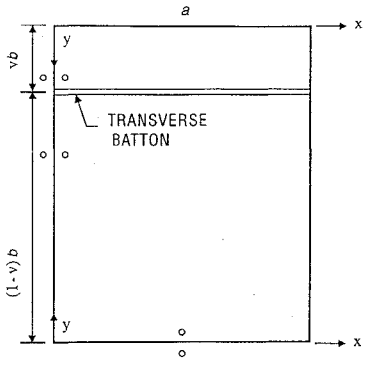

Fig. 4 Coordinate systems utilized in analysing quarter segment of the membrane.

Consider the motion of the membrane segments. The differential equation governing membrane motion is written as

$$\frac{\partial^2 w(x, y)}{\partial y^2} + \left(\frac{\omega}{c}\right)^2 w(x, y) = 0 \tag{1}$$

with $w(x, y)$ in the form

$$w(x, y) = \sum_{m=0,1}^{\infty} Y_m(y) \cos \frac{m\pi x}{a} \tag{2}$$

There is zero tension in the x direction, and in view of the boundary conditions only the first trigonometric term on the right-hand side of Eq. (2) needs be retained. Substitution for $Y_m(y)$ in the differential equation yields the general solution

$$Y_m(y) = C_{1m} \sin \beta y + C_{2m} \cos \beta y \tag{3}$$

where $\beta^2 = (\omega/c)^2$, and C_{1m} and C_{2m} are constants to be determined.

Utilizing the subscripts 1 and 2 now to refer to the upper and lower segments of the membrane, and enforcing the boundary conditions at $y = 0$

$$Y_{1m}(y) = C_{1m} \sin \beta y \tag{4}$$

and

$$Y_{2m}(y) = C_{2m} \cos \beta y \tag{5}$$

Enforcing the condition of continuity of the membrane at the batten requires

$$C_{2m} = C_{1m}\theta_1 \tag{6}$$

where

$$\theta_1 = \sin(\beta' v)/\cos(\beta' v^*) \tag{7}$$

and $\beta' = \beta b$, and $v^* = 1 - v$.

Equating the forces per unit length at the batten

$$T\left[\frac{dY_{1m}(y)}{dy}\bigg|_{y=vb} + \frac{dY_{2m}(y)}{dy}\bigg|_{y=v^*b}\right] = -\frac{P}{a} \tag{8}$$

or

$$C_{1m}\beta[\cos \beta' v - \theta_1 \sin \beta' v^*] = (-P/aT) \tag{9}$$

and, therefore,

$$C_{1m} = \frac{Pb}{aT\beta'[\cos \beta' v - \theta_1 \sin \beta' v^*]} \tag{10}$$

The dynamic equilibrium condition requires that the force acting on the bar must equal the product of its mass and acceleration. This leads to the equality

$$P = \frac{A_{mB}\rho ab\omega^2 Pb \sin \beta' v}{aT\beta'[\cos \beta' v - \theta_1 \sin \beta' v^*]} \tag{11}$$

Introducing the eigenvalue $\lambda^2 = \omega a/c$ and recalling that $c = \sqrt{T/\rho}$, Eq. (11) may be rewritten as

$$P\left(1 - \frac{A_{mB}\lambda^4\phi^2 \sin \beta' v}{\beta'[\cos \beta' v - \theta_1 \sin \beta' v^*]}\right) = 0 \tag{12}$$

A search for those values of λ^2 which cause the quantity in braces of Eq. (12) to vanish provides the eigenvalues for the fully symmetric modes of vibration of the membrane. From each eigenvalue λ^2, a value for the associated circular frequency ω may be computed, which in turn permits evaluation of each β. The mode shape associated with each eigenvalue can thus be determined.

Modes Antisymmetric About the Long Central Axis and Symmetric About the Other Axis

Computation of the eigenvalues for this family of modes is slightly more complicated. Again, only the upper right-hand quadrant of the membrane is analyzed. This quadrant is shown in Fig. 4.

There must be zero displacement along the edge $x = 0$. As a result, the solution is taken in the form

$$w(x, y) = \sum_{m=1,3}^{\infty} Y_m(y) \sin \frac{m\pi x}{2a} \tag{13}$$

Enforcing the appropriate boundary conditions, the solutions for the functions $Y_m(y)$ take on a form identical to that given by Eqs. (4–7) for the symmetric modes.

Let the distributed force exerted by the membrane on the batten be represented in series form as

$$p(x) = \sum_{m=1,3}^{\infty} E_m \sin \frac{m\pi x}{2a} \tag{14}$$

Then

$$T\left[\frac{dw_1(x, y)}{dy} + \frac{dw_2(x, y)}{dy}\right]\bigg|_{y=vb} = -p(x) \tag{15}$$

or, on substituting for $w_1(x, y)$ and $w_2(x, y)$

$$TC_{1m}\beta[\cos \beta v b - \theta_1 \sin \beta v^* b] = -E_m \tag{16}$$

Therefore,

$$C_{1m} = \frac{-E_m b}{T\beta'[\cos \beta' v - \theta_1 \sin \beta' v^*]} \tag{17}$$

Along the contact line between the batten and the membrane the displacement must be a linear (ramp) function of x. Denote this displacement as $B(x)$ with

$$B(x) = Bx \tag{18}$$

This function is also expanded in the same sine series as utilized in Eq. (14) to obtain

$$Bx = \sum_{m=1,3}^{\infty} B_m \sin \frac{m\pi x}{2a} \tag{19}$$

where

$$B_m = \frac{8Ba}{(m\pi)^2} \sin \frac{m\pi}{2} \tag{20}$$

The constraining equations relating the unknown coefficients of the problem are now developed. Consider, first, the dynamic equilibrium of the rotating batten and write

$$I\frac{d^2}{dt^2}\left\{\frac{dw_1(x, y)}{dx}\right\}\bigg|_{y=ub} = \int_0^a p(x) \cdot x \, dx \tag{21}$$

Denoting I as $A_{MI}\rho a^3 b$, and obtaining the slope, $dw_1(x, y)/dx$, from Eq. (18), then from Eq. (21)

$$A_{MI}\rho a^3 b\omega^2 B = \sum_{m=1,3}^{\infty} \frac{4E_m a^2}{(m\pi)^2} \sin\frac{m\pi}{2} \tag{22}$$

or, introducing λ^2,

$$A_{MI}BTa\lambda^4\phi^2 = \sum_{m=1,3}^{\infty} \frac{4E_m b}{(m\pi)^2} \sin\frac{m\pi}{2} \tag{23}$$

Utilizing k terms in the preceding series there are $k+1$ unknowns which are designated as BTa, and $E_m b$, m taking on k successive values. Equation (23) provides an algebraic homogenous equation relating these $k+1$ unknowns.

The remaining constraint states that the displacement along the bar must equal $B(x)$. Accordingly, each term of Eq. (13) is equated with the corresponding term of Eq. (19), utilizing also Eqs. (17) and (20). This gives rise to a set of k homogeneous algebraic equations.

For any m

$$\frac{-E_m b \sin\beta' v}{T\beta'[\cos\beta' v - \theta_1 \sin\beta' v^*]} = \frac{8Ba}{m\pi^2} \tag{24}$$

or

$$\frac{-E_m b \sin\beta' v}{\beta'[\cos\beta' v - \theta_1 \sin\beta' v^*]} = \frac{8BaT}{m\pi^2} \tag{25}$$

Equations (23) and (25) provide the required $k+1$ homogenous algebraic equations relating the unknowns BaT, and $E_m b$. From these equations the eigenvalue matrix for the problem may be constructed and the eigenvalues and mode shapes computed.

Remaining Mode Families

A further set of modes are those symmetric about the long axis and antisymmetric about the short axis. A brief review of the mathematical procedure dealing with fully symmetric modes reveals that the analysis therein is readily modified for this problem. It is only necessary to replace the cosine functions utilized in the solution for the functions $Y_m(x)$ with sine functions [Eq. (5)]. The mathematical procedure of the latter section may also be modified in a similar fashion for modes which are antisymmetric about both the membrane central axes.

Finite Element Approach

The rectangular membrane was also modeled using the finite element approach. Two different end-beam total thicknesses [4.76 mm (0.1875 in.) and 6.35 mm (0.25 in.)] were modeled, and both were analyzed with and without the effects of gravity. The nodal organization of the membrane structure is shown in Fig. 5. All of the degrees of nodes 1–5 were anchored, and downward loads were applied on nodes 314–318. Additional runs were carried out on the 4.76-mm (0.1875-in.) total thick end-beam case assuming a uniform stress distribution and zero structural stiffness in the membrane for the purpose of comparing the FEM results with the CMM results.

Custom designed (in-house) software was used to analyze the normal modes of the preloaded membrane structure. Because of the very low structural stiffness in the out of-plane direction, "negative" geometric stiffness caused by compression in one of the principal directions creates regions of static instability, characterized by wrinkled areas in the membrane. This instability eliminated the possibility of using commercially available finite element programs, such as Nastran, because they do not include the facilities required to overcome this instability.

To solve for the normal modes of the tensioned membrane, a linear static stress analysis is performed to determine the stress distribution. To superimpose the effects of gravity on the loading, simple discrete downward forces were applied at the nodes. Since the nodal density was quite high, it was assumed that this was an adequate approximation. The stress data which are recovered from this isoparametric solution are only accurate at the integration point of

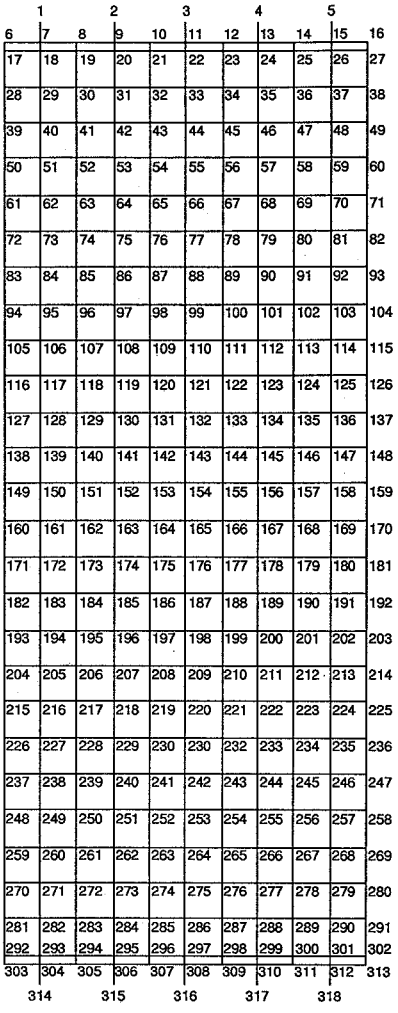

Fig. 5 Nodal organization of the membrane for finite element analysis.

the elements, which are the element centers. Later, for the calculation of the geometric stiffness, a bilinearly varying stress is used, requiring the state of stress at each node. Therefore, by spline fitting the element center stresses to a smooth surface over the entire membrane, the nodal stresses can then be calculated. This increases the accuracy of the geometric stress in the membrane, especially where compression is detected.

To solve the problem of negative stiffness in the regions of compression, the stress distribution is adjusted before the geometric stiffness matrices are calculated. The principal stresses at the nodes are tested. If the minimum stress is negative, it is changed to zero. Then the axial and shear stresses are recalculated using the same maximum principal stress and its angle to the axial direction. In this way, the original tensile stress and its direction are retained. Furthermore, since the custom software uses bilinearly varying stress in the elements, if only one or two nodal stresses need compression relaxation in an element, the overall stress distribution in the element more closely resembles the original state than had the stress field been represented as a constant in each element. In the event that both principal stresses are negative, the stresses are set to zero at that node. If this trend is widespread, the problem is of particularly poor choice, and one can not expect to obtain reasonable modal data. Because for the most part the membrane is in tension, this compression relaxation does not change the overall stress distribution significantly but eliminates the instability which prevents the analysis from being possible in Nastran.

To verify that the nodal density was adequately high, simple h-convergence tests were performed. Considering the regularity of the structure, the number of nodes was quite large, which served to provide many comparison points for the CMM model. By increasing number of widthwise nodes from 11 to 13, and number of lengthwise nodes from 26 to 31, creating an overall increase from 318 to 441, the

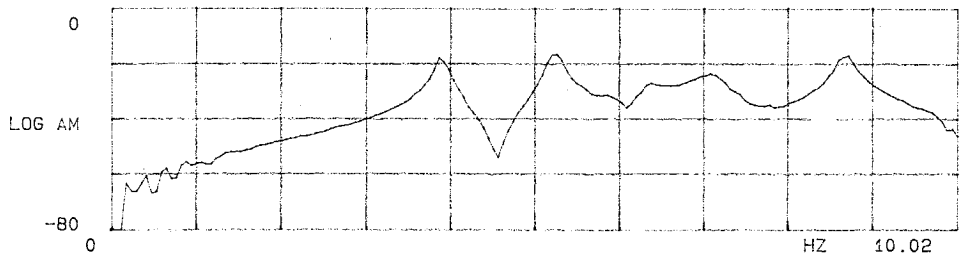

Fig. 6 Typical frequency response function from in-air modal tests.

frequency drop in mode 1 was only 0.101%, and in mode 2 was only 0.141%. This indicates that the nodal spacing was sufficiently fine.

Modal Tests of the Membrane

Modal tests, both in air and in vacuum, were performed. As mentioned earlier, one of the objectives of these tests is to determine frequencies and mode shapes of a uniformly tensioned rectangular membrane to verify experimentally the analytical models just described.

Modal Tests on the Support Frame

Before the in-air modal tests were performed on the membrane, some modal tests on the support frame were performed. Since the membrane was mounted on the frame (as shown in Fig. 2), it was essential that the frame be quite rigid. Effectively, this means that the resonant frequencies of the frame are required to be well separated from those of the membrane. Since only out-of-plane deflections are considered relevant for the membrane, it is of prime importance that the first out-of plane resonant frequency of the frame alone should be well separated from the first frequency of the membrane. The frame was attached firmly to the rails on a 366 tonne (806883.6 lb) seismic block. To find the first out-of-plane frequency of the frame, modal tests were performed using an impact hammer. Piezoelectric accelerometers were mounted at several locations on the frame. The first out-of-plane mode of the frame was found to have a frequency at about 30.9 Hz. This frequency is reasonably well separated from the fundamental frequency (about 9 Hz) of the membrane.

Excitation Tests

After the modal testing of the frame, the membrane was mounted into its support frame. A series of excitation tests (in air) on the membrane were carried out. The purpose of the excitation tests was to identify an suitable excitation system together with the most suitable number of exciters, exciter locations, and the types and levels of excitation for the performance of modal tests on the membrane.

The excitation tests consisted of applying excitation of continuous/burst random inputs over the frequency bandwidth of interest (up to 30 Hz) to either a single point or to multiple points on the lower batten of the membrane. The resultant dynamic responses, subsequently in the form of frequency response functions, of a sufficient number of points on the membrane were recorded using a single-channel laser vibrometer. The analog output data (velocity signal) of the laser were acquired directly using Leuven Measurement Systems- (LMS-) FMON[3] software of the LMS modal system. Different excitation techniques using varying excitation levels at different input locations were applied and examined.

Based on these excitation tests it was concluded that one exciter was sufficient to excite at least the first two modes of vibration of the membrane. Either type of excitation, continuous or burst random, was found suitable. A suitable excitation level was also recorded.

In-Air Modal Tests of the Membrane

Following the excitation tests, the in-air modal tests on the membrane were performed. The membrane was subjected to the desired loading [364.83 N/m (25 lb/ft)] which was achieved by applying a 66.72 N (15 lb) load at each of the five springs.

Only one exciter was used. It was supported on a pump dolly. The excitation input location was on the lower batten (as shown in Fig. 2). The excitation input signal to the power amplifier was selected as continuous random with a frequency range of 0–30 Hz. The excitation forces were applied in only one direction, that is, normal to the surface of the test membrane. Two single-channel laser vibrometers were used to measure the dynamic responses of the membrane, thus providing two measurement points (locations) simultaneously. To identify the associated mode shapes of the membrane, it was considered appropriate to measure the response at 45 locations. Laser-light reflecting targets were mounted at these locations. The structural dynamic responses (velocity signals) from the two lasers, along with the force input into the membrane, were acquired by the LMS modal system using LMS-FMON software to yield frequency response functions (FRFs-velocity/force). FRFs were obtained using 25 measurement averages. These FRFs were analyzed using LMS-SMAP[4] software to yield the modal parameters.

Table 1 Modal frequencies of the test membrane

Mode	Experimental, Hz		Theoretical, Hz in vacuum	
	in air	in vacuum	FEM	CMM
1	3.89	8.78	9.21	9.01
2	5.24	9.16	9.57	9.85

Results From In-Air Modal Tests

The experimental frequencies of the first two modes of the membrane were found to be 3.89 Hz and 5.2 Hz (as shown in Table 1). A typical FRF is shown in Fig. 6. The associated mode shapes are shown in Fig. 7. From the mode shapes it is clear that the first mode is a fully symmetric mode, and second mode is antisymmetric about the long axis and symmetric about the short axis. On comparing these two measured frequencies for the first two modes, in Table 1, with the corresponding theoretical values as yielded by the CMM and the FEM, it is noted that the experimental values are much lower than the corresponding predicted values. This is due to aerodynamic effects. The analytical results do not account for such effects and are valid in vacuum only. These results make it clear that it is essential that the tests be carried out in vacuum.

In-Vacuum Tests of the Membrane

The membrane within its mounting frame was firmly attached to the support platform in a thermal vacuum chamber (TVC). In the in-air modal tests, the membrane frame was attached to a seismic block. To investigate the effect of change in boundary conditions on the modal parameters, the in-air modal test was repeated on the membrane while in the TVC. As before, only one exciter was used. No significant differences in the values of the modal frequencies were obtained for the two slightly different boundary conditions.

For the in-vacuum tests, only one laser vibrometer was used. Furthermore, because after each measurement (i.e., one location) the TVC would have to be back filled to move the laser to focus on another target, because of time and cost constraints it was only considered practical to measure the response at one suitable point. Thus, in vacuum only modal frequencies were identified. No mode shapes were obtained. The measured frequency response function is shown in Fig. 8. The first two modal frequencies from in-vacuum tests are also given in Table 1 as well as those predicted through analysis. There is a reasonable agreement between the experimental and theoretical values.

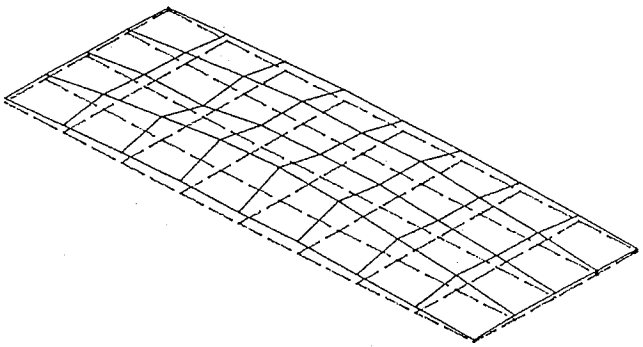

MODE 1 (f=3.89 Hz)

a)

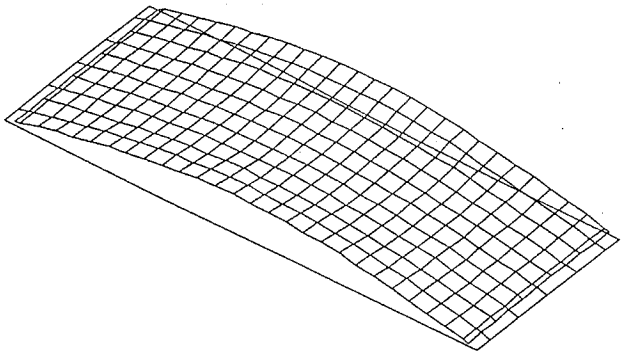

MODE 1 (f=9.21 Hz)

c)

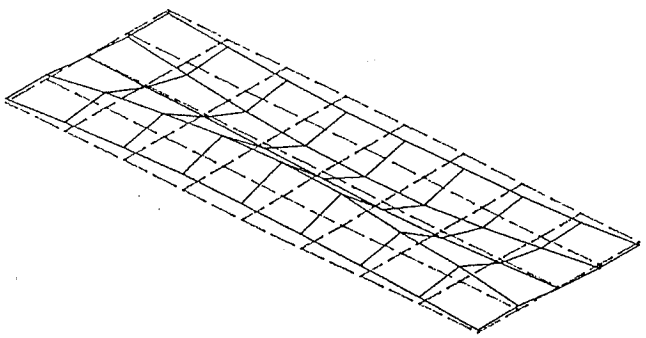

MODE 2 (f=5.24 Hz)

b)

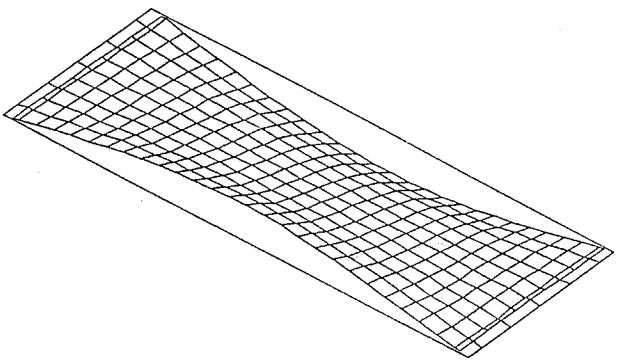

MODE 2 (f=9.57 Hz)

d)

Fig. 7 Experimental and FEM mode shapes of the membrane: a) and b) measure mode shapes; c) and d) computed mode shapes.

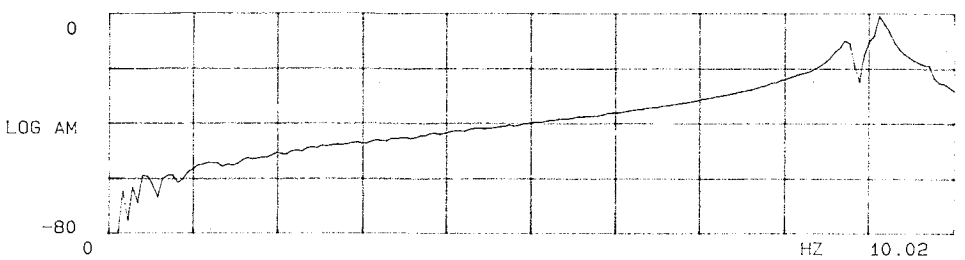

Fig. 8 Typical frequency response function from in-vacuum modal tests.

Discussion and Conclusions

The project described constitutes completion of the first phase of work devoted to developing reliable testing methods and theoretical techniques for free vibration behavior of tensioned membranes. The principal complication in the present test membrane is related to the utilization of rigid bars which not only impart tension to the main body of the membrane but also participate in its vibrating motion.

The effects of atmospheric air on membrane natural frequencies are substantial (see Table 1). The theoretical studies performed in this work give quite good agreement with experimental frequencies measured in vacuum.

The ultimate membrane of interest is the LADD membrane. In this case, there are a number of further complicating effects. One of these is the existence of a significant variation in tension along the membrane, since it is deployed in a vertical plane and there is significant mass in the membrane material. Another is the existence of non-negligible membrane flexural stiffness due to the existence of a grid of transceiver modules attached to both sides of the membrane. With the first phase of the work completed an experimental and analytical study is now underway with the goal of incorporating these additional complicating effects into the experimental and analytical analyses.

Acknowledgments

The authors wish to acknowledge R. Hafer, SBR Project Manager, of the Department of National Defence, for supporting and funding this research activity. The authors would also like to thank R. Gawlik for his help during tests. The tests were carried out at the David Florida Laboratory of the Canadian Space Agency in Ottawa.

References

[1]Pugh, M. L., Denton, R. J., Jr., and Strange, T. J., "The Development and Testing of the Lens Antenna Deployment Demonstration (LADD) Test Article," *Proceedings 5th NASA/DOD Control-Structures Interaction Technology Conference* (Lake Tahoe, NV), NASA Conf. Pub. 3177, March 1992, pp. 153–160.

[2]Gorman, D. J., and Singhal, R. K., "Free Vibration Analysis of Rectangular Membranes with Local Attached Masses and Rigid Transverse Anchorage Bars," *Proceedings 2nd ESA Workshop—Modal Representation of Flexible Structures by Continuum Methods*, European Space Research and Technology. Noordwijk, The Netherlands, European Space Agency ESA WPP-034, June 1992, pp. 311–327.

[3]Anon., "LMS-FMON User Manual," Leuven Measurement and Systems, Heverlee, Belgium, Oct. 1986.

[4]Anon., "LMS-SMAP User Manual," Leuven Measurement and Systems, Heverlee, Belgium, Oct. 1986.